Astronomy & Astrophysics manuscript no. Giommi1OUSXB˙paper4arXiv
March 14, 2022
© ESO 2022

arXiv:1904.06043v1 [astro-ph.HE] 12 Apr 2019

Open Universe for Blazars: a new generation of astronomical products based on 14 years of Swift-XRT data.

P. Giommi[1,2,3], C.H. Brandt[3,4], U. Barres de Almeida[5,3], A.M.T. Pollock[6], F. Arneodo[7], Y. L. Chang[3], O. Civitarese[8,9], M. De Angelis[1], V. D'Elia[10,12], J. Del Rio Vera[11], S. Di Pippo[11], R. Middei[13], A. V. Penacchioni[8], M. Perri[10,12], R. Ruffini[3], N. Sahakyan[14], and S. Turriziani[15]

[1] Italian Space Agency, ASI, via del Politecnico snc, 00133 Roma, Italy
[2] Institute for Advanced Study, Technische Universität München, Lichtenbergstrasse 2a, D-85748 Garching bei München, Germany
[3] ICRANet, P.zza della Repubblica 10, 65122, Pescara, Italy
[4] Jacobs University, Physics and Earth Sciences, Campus Ring 1, 28759, Bremen, Germany
[5] Centro Brasileiro de Pesquisas Físicas, Rua Dr. Xavier Sigaud 150, 22290-180, Rio de Janeiro, Brazil
[6] Department of Physics and Astronomy, University of Sheffield, Hounsfield Road, Sheffield S3 7RH, England
[7] New York University Abu Dhabi, Abu Dhabi, UAE
[8] Institute of Physics. IFLP-CONICET. diag 113 e/63-64.(1900) La Plata. Argentina
[9] Department of Physics. University of La Plata. 49 and 115.C.C.67 (1900) La Plata, Argentina
[10] Space Science Data Center, SSDC, ASI, via del Politecnico snc, 00133 Roma, Italy
[11] United Nations Office for Outer Space Affairs, UNOOSA, Vienna, Austria
[12] INAF - Osservatorio Astronomico di Roma, via Frascati 33, I-00040 Monteporzio Catone, Italy
[13] Dipartimento di Matematica e Fisica, Università degli studi Roma Tre, Via della Vasca Navale 84, 00146, Roma, Italy
[14] ICRANet-Armenia, Marshall Baghramian Avenue 24a, Yerevan 0019, Armenia.
[15] Computational Astrophysics Laboratory - RIKEN, 2-1 Hirosawa, Wako, Saitama 351-0198, Japan
e-mail: paolo.giommi@asi.it

Preprint online version: March 14, 2022

ABSTRACT

Aims. Open Universe for blazars is a set of high-transparency multi-frequency data products for blazar science, and the tools designed to generate them. Blazars are drawing growing interest following the consolidation of their position as the most abundant type of source in the extragalactic very-high energy γ-ray sky, and because of their status as prime candidate sources in the nascent field of multi-messenger astrophysics. As such, blazar astrophysics is becoming increasingly data driven, depending on the integration and combined analysis of large quantities of data from the entire span of observational astrophysics techniques. The project was therefore chosen as one of the pilot activities within the United Nations Open Universe Initiative.

Methods. We aim to deliver innovative data science tools for multi-messenger astrophysics. In this work we developed a data analysis pipeline called *Swift-DeepSky* based on the Swift XRTDAS software and the XIMAGE package, encapsulated into a Docker container. *Swift-DeepSky* downloads and reads low-level data, generates higher-level products, detects X-ray sources and estimates several intensity and spectral parameters for each detection, thus facilitating the generation of complete and up-to-date science-ready catalogues from an entire space-mission dataset. The Docker version of the pipeline – whose concept can be reproduced with other missions – and its derived products is publicly available from the Open Universe Website at openuniverse.asi.it

Results. We present the results of a detailed X-ray image analysis based on *Swift-DeepSky* that was run on all Swift XRT observations including a known blazar, carried out during the first 14 years of operations of the Neil Gehrels Swift Observatory. Short exposures executed within one week of each other have been added to increase sensitivity, which ranges between $\sim 1 \times 10^{-12}$ and $\sim 1 \times 10^{-14}$ erg cm^{-2} s^{-1}(0.3-10.0 keV). After cleaning for problematic fields, the resulting database includes over 27,000 images integrated in different X-ray bands, and a catalogue, called 1OUSXB, that provides intensity and spectral information for 33,396 X-ray sources, 8,896 of which are single or multiple detections of 2,308 distinct blazars. All the results can be accessed on-line in a variety of ways: e.g., from the Open Universe portal at openuniverse.asi.it, through Virtual Observatory services, via the VOU-Blazar tool and the SSDC SED builder. One of the most innovative aspects of this work is that the results can be safely reproduced and extended by anyone.

Key words. galaxies: active – X-rays:galaxies – Methods: data analysis – Astronomical data bases:catalogs

1. Introduction

Providing open and transparent access to scientific data is a social obligation of the scientific community, and central to the progress of research in the era of big data and of data-driven science. Facilitated access to scientific data can also play a critical role in education, capacity building, and in the promotion of citizen science. For this reason the United Nations recognised that free access to space-science data is

a strategic objective contributing to the achievement of the Sustainable Development Goals (SDGs)[1].

In the field of astronomy, the third United Nations Conference on the Exploration and the Peaceful Uses of Outer Space, UNISPACE III, requested action to be taken to improve scientific knowledge of near and outer space by promoting cooperative activities in such areas as astronomy, space biology and medicine, space physics, the study of near-Earth objects, and planetary exploration. This request is echoed in "Open Universe".

"Open Universe"[2] (Giommi et al. 2018) is an initiative proposed by Italy to the United Nations Committee on the Peaceful Uses of Outer Space (COPUOS) in 2016[3] that is now being actively developed by a number of countries in coordination with the UN Office for Outer Space Affairs (UNOOSA). Its main goal is to contribute in making astronomy and space-science data more openly available, easily discoverable, free of bureaucratic, administrative or technical barriers, and therefore usable by the widest possible community, from professional researchers to all people interested in space science. In doing so, Open Universe aims to support an increase in productivity of space research, facilitate the emerging field of data-driven science, and stimulate a significant acceleration towards the democratisation of space science and the benefits therefrom.

Open access to scientific data, and its associated technologies, has been actively addressed by a number of initiatives working in complementary ways, such as the International Virtual Observatory Alliance (IVOA) [4], the European Open Science Cloud (EOSC)[5], the Research Data Alliance (RDA)[6], the Astronomy ESFRI and Research Infrastructure Cluster (ASTERICS)[7], among others.

Starting from different angles and approaches, these various initiatives propose and develop solutions to support the reuse of astrophysical data, following general concepts which are now commonly accepted and widely endorsed, as expressed, for example, in the FAIR Guiding Principles for Scientific Data Management and Stewardship (Wilkinson et al. 2016) and in the particular application of the FAIR principles in astronomy and space science (Pollock 2018).

The Open Universe Initiative stresses that open data by itself does not equal data transparency, which, in our view, requires compliance to all of the following criteria: a) satisfy the FAIR principles; b) optimise the scientific and sociological value of the data; c) provide access via the simplest possible interfaces; and d) require no additional processing.

In line with this general vision and, in particular, with the democratisation of science and its potential as a tool for development, Open Universe wishes to contribute to offering accessible space science data that can be used by anyone, and that can be flexibly employed in different applications from research to education, thus responding to the global demand for transparency of all goods produced through public funding. Currently, the operational part of Open Universe can be accessed through its data portal (openuniverse.asi.it), which acts as a window to web-based initiatives collecting data. The portal provides also a few additional online functions for smart, purpose-built data mining and data visualisation, such as the "VOU-Blazars" and "VOU-SED" tools. The Initiative, however, is not limited to such services, but aims to the continuous development of new data products and data-oriented solutions. It is open to collaboration with all countries and institutions sharing our views on data transparency and open science, and willing to participate in activities to increase the reach of astronomical datasets, and lower the technical complexity required to work with them.

As a first concrete application of this view, we present "Open Universe for Blazars", a project devoted to the generation of transparent scientific products from multi-frequency astronomical data by the Neil Gehrels Swift Observatory (Gehrels et al. 2004, hereafter Swift) and other astronomy satellites.

This first project, developed as a pilot activity within the Initiative, focuses on blazars, astrophysical sources that are receiving increased attention as they are expected to abound in upcoming very high-energy γ-ray sky surveys[8] [9]. In addition, blazars will likely play a crucial role in the nascent field of multi-messenger astrophysics, following their recent potential association with astrophysical high-energy neutrinos and Ultra High Energy Cosmic Rays (UHECRs, e.g. IceCube Collaboration et al. 2018; Resconi et al. 2017)

The multi-messenger and big data characteristics of blazar research motivated the project as a test-bed for the incorporation of novel computational technologies to increase data transparency and usability. To that end, we pioneered the combination of Virtual Observatory services with Linux containers to provide enhanced accessibility to top-quality, reliable scientific data products on demand, with minimum recourse to mission-specific data reduction techniques, or computational knowledge by the user.

Linux Containers, and in particular the implementation by Docker Inc.[10], provide a portable solution for shipping software. As shown below, this technology is suitable for a safe and robust distribution of ready-to-use complex astronomical data analysis packages, with a simple user interface, removing the need for a high-degree of specialised knowledge that would otherwise be required. This in turn opens the way to a number of flexible applications, such as in distributed and web-based intensive data analysis, mobile-compatible operation, and improved usability by non-experts for purposes of science, education or citizen science.

2. Blazars and the Swift Observatory

Blazars are a special and uncommon type of Active Galactic Nucleus[11] (AGN, Padovani et al. 2017), distinguished by

[1] http://www.unoosa.org/oosa/oosadoc/data/documents/2018/aac.105/aac.1051175_0.html
[2] http://openuniverse.asi.it
[3] http://www.unoosa.org/res/oosadoc/data/documents/2016/aac_1052016crp/aac_1052016crp_6_0_html/AC105_2016_CRP06E.pdf
[4] http://www.ivoa.net
[5] https://www.eosc-portal.eu
[6] https://www.rd-alliance.org
[7] https://www.asterics2020.eu/
[8] https://www.cta-observatory.org/wp-content/uploads/2017/11/ScienceWithCTA_FINAL2_updated.pdf
[9] http://english.ihep.cas.cn/lhaaso
[10] https://www.docker.com
[11] only one every $\sim$ 350 objects listed in current catalogues of AGN is a blazar. See Sect. 3

the emission of highly variable radiation across the entire electromagnetic spectrum. It is commonly accepted that a large part of this radiation is generated by charged particles within a jet of material that moves away at relativistic speeds from the central supermassive black hole and happens to be pointing in the direction of the Earth (see e.g. Urry & Padovani 1995).

Blazars come in two sub-classes, FSRQs and BL Lacs, depending on their optical spectra: FSRQs show broad emission lines just like normal QSOs, while BL Lacs instead display at most weak emission lines, sometimes exhibit absorption features, and in many cases are completely featureless. The observational appearance of blazars depends on a complex mix of physical and geometrical conditions, and their classification is subject to selection effects (Giommi et al. 2012).

The Spectral Energy Distribution (SED, a plot of the $\nu f(\nu)$ flux as a function of frequency ν) of blazars is characterised by a "double humped" shape (see e.g. Fig 1 of Padovani et al. 2017, or Fig. 5 and Fig. 7 below). The low-energy component, peaking between the IR and the X-ray band, is generally attributed to synchrotron radiation produced by relativistic electrons moving in a magnetic field. The second component extends well into the γ-ray band, and is typically explained as either inverse Compton scattering of the electrons against photons, or other radiation mechanisms involving hadronic scenarios and neutrino emission.

Despite their rarity compared to other types of AGN, the particular radiation processes that cause blazars to emit across the entire electromagnetic spectrum and the particular geometrical circumstances that cause strong flux amplification, make these objects the most common type of extragalactic source so far detected in the microwave and γ-ray skies. Blazars have also been associated with high-energy astrophysical neutrinos (e.g. Mannheim 1995; Padovani et al. 2018) and possibly to Ultra High Energy Cosmic Rays (e.g. Resconi et al. 2017). For the same reason, blazars are expected to be found in large numbers in the high-energy extragalactic sky that will soon be surveyed by the new generation of powerful VHE observatories such as CTA, HAWK or LHAASO, and will likely play a crucial role in the emerging field of multi-messenger astrophysics.

Blazar research has always been central to the scientific program of the Swift observatory (Gehrels et al. 2004), which is a NASA mission launched in 2004 November and still fully operational. The Swift hardware and software were built by an international collaboration involving US, Italy, and United Kingdom. The original main scientific driver of the Swift mission was to detect gamma-ray bursts (GRBs) in the hard X-ray band with the Burst Alert Telescope (BAT, Barthelmy et al. 2005), and quickly follow-up their emission at longer wavelength with the X-Ray Telescope (XRT, Burrows et al. 2005), and the Ultraviolet/Optical Telescope (UVOT, Roming et al. 2005). Although specifically designed to carry out GRB science, Swift has proven to be an extremely effective multi-purpose multi-frequency observatory. During its first 14 years of operations, the satellite carried out over 24,000 pointings [12] of approximately 2,600 catalogued blazars, for a total of 44.6 Ms of XRT net exposure time, corresponding to ≈ 14% of the entire mission scientific program. The XRT is an X-ray telescope with a CCD at its focus that is normally operated in either of two readout modes, Photon Counting (PC) mode, which provides full imaging and spectral information, routinely used to observe targets that are faint or moderately bright X-ray sources, and Windowed Timing (WT) mode, that does not provide full imaging information and is used to measure the X-ray spectrum and the time variability of sources brighter than $\approx 2 \times 10^{-11}$ erg cm^{-2} s^{-1} in the 0.3-10.0 keV band.

Fig. 1 plots the amount of XRT exposure time dedicated to observations of blazars in PC mode during the first 14 years of Swift operations. The distribution of exposure times of individual XRT pointings, each characterised by an 11 digit unique identifier called Observation_ID or sequence number, ranges from a few hundred seconds to about 10 ks, with a clear peak at 1 ks (see fig. 2).

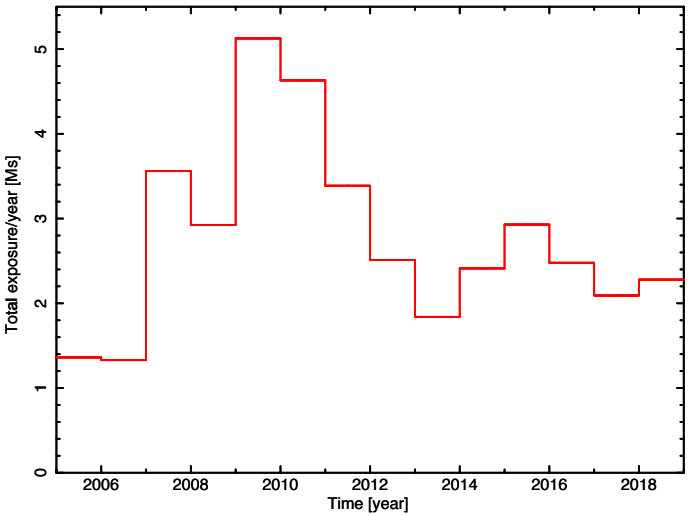


Fig. 1. The distribution of XRT exposure time in PC mode dedicated to known blazars over the 14 years of Swift mission operations covered by this work.

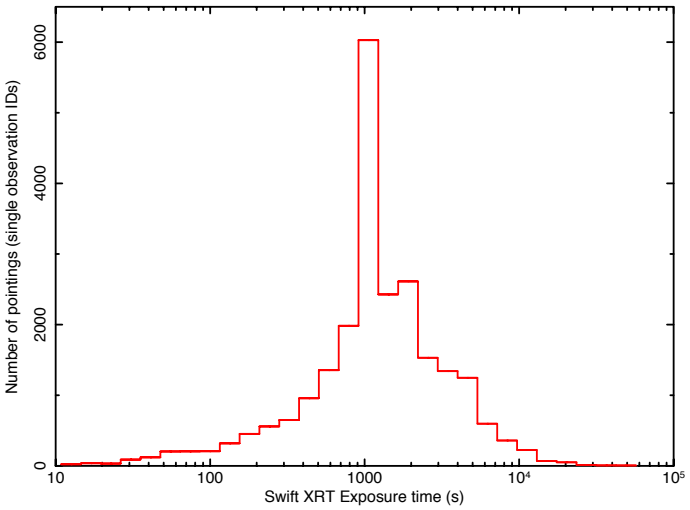


Fig. 2. The distribution of Swift exposure times of single Observation_ID pointings where the XRT field of view includes a known blazar. Note the strong peak at 1 ks.

[12] here we consider only single observations_ids with XRT exposures larger than 200 seconds in PC readout mode

All Swift data immediately enter the public domain and are openly available to anyone. The official Swift archives provide access to low and intermediate level data products together with complex reduction and analysis software and calibration files, designed to be used by experienced scientists to conduct higher-level data processing. To benefit fully of the Swift data, non-experts in the field would have to go through a learning process that most people cannot afford. Even professionals may have significant problems if they have no direct experience with X-ray data analysis or need to analyse large amounts of data, like hundreds of observations.

Following the directives of data transparency described in the previous section, the work presented here builds on the public domain data provided by Swift to deliver science-ready, high-level products for the instrument's entire blazar catalogue, increasing its usability to a larger number of potential users. This work is meant to be a concrete example of how the Open Universe Initiative can contribute to create effective solutions to data accessibility. Such efforts in turn hold a potential impact for research in various sectors of astrophysics and space science, and in the development of new, more user-oriented applications.

3. A master list of blazars

Most blazars known to date have been found in radio, X-ray, or γ-ray surveys, or through multi-frequency searches, with a discovery rate that has been steadily increasing over the last several years. For this reason no recent complete lists exist. To assemble a reasonably up-to-date comprehensive catalogue of blazars we have combined the BZCAT 5th edition (Massaro et al. 2015), the list of blazars in the Fermi 3LAC catalogue (Ackermann et al. 2015) and the recently released 3HSP list of high energy peaked and extreme blazars (Chang et al. 2019a).

The resulting master list includes 5340 distinct objects, a number that might seem large since only 20 years ago just a few hundred blazars were known. However, the comparison with the almost 2 million catalogued QSOs (see the million quasars catalogue V5.7; Flesch 2015)[13] gives a clear measure of how rare blazars are compared to other AGN. Despite that, blazars are almost the only type of extragalactic source detected so far in the high energy γ-ray band, reflecting their highly energetic and extreme nature.

To determine how many blazars have been observed by Swift during its first 14 years of orbital operations, we have cross-matched our master catalogue of blazars with the list of all Swift-XRT observations carried out before 31 December 2018, using a matching radius of 12 arc-minutes, approximately the size of the XRT field-of-view. About 50% of the blazars in our master list (2633 objects) are within the field-of-view of at least one XRT observation. If we consider only pointings carried out in PC mode with exposure of at least 200 seconds, this number reduces to 2585.

While most blazars have been observed just once or a few times, several have been observed repeatedly, up to over 1,000 times for the case of MRK 421 (in PC or WT mode), for a total of approximately 18,000 XRT exposures in PC mode. For technical reasons, Swift observations of a given target are frequently split into short exposures (corresponding to single OBS_ID, typically of 1 ks each, see fig. 2) repeated over a period of a few days, until the requested exposure time is reached. In an effort to represent the originally requested exposure times, typically between 3 and 10 ks, and to increase sensitivity, rather than single snapshots or observation IDs we have merged into a single "observation" all the exposures carried out within one week of each other. This merging procedure reduced to 11,399 the number of observations of blazars to be processed as described the next paragraph.

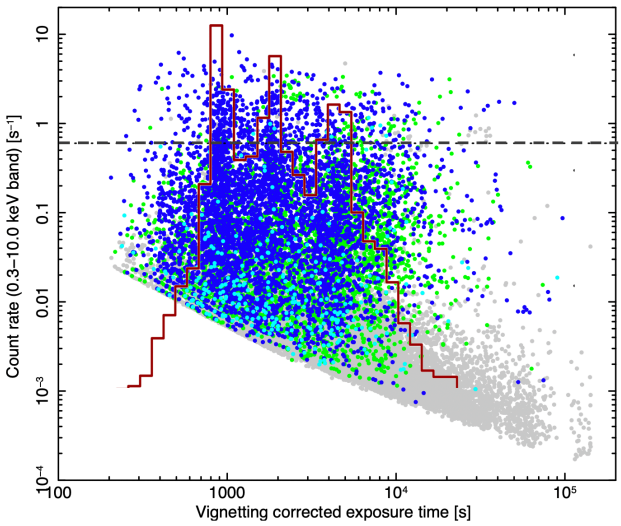


Fig. 3. Plot of the count rate in the 0.3-10.0 keV band versus the vignetting-corrected exposure time for all the sources detected in the data-set considered. FSRQs: blue points ; BL Lacs: green points; other targets and serendipitous sources: light grey points. The dotted horizontal line marks the count-rate limit above which pileup problems become significant in data taken in PC mode. The red histogram represents the number of blazars in each time bin, showing three peaks at approximately 1, 2 and 4-5ks, the preferred exposure times for blazars.

4. Data processing

To perform a detailed Swift-XRT image analysis of the blazars in the sample described above, we have developed a software pipeline called *Swift-DeepSky* (Brandt et al. 2019) building on the Swift X-Ray Telescope Data Analysis Software (XRTDAS), designed and developed under the responsibility of the Space Science Data Center (SSDC) of the Italian Space Agency (ASI) and distributed within the NASA HEASoft[14] software package and related XRT calibration files (CALDB)[15]. For a description of the *Swift-DeepSky* software see Appendix A.

The processing of all the 11,399 one-week co-added Swift XRT PC mode observations of the blazars described in Section 3 led to the detections of approximately 51,000 X-ray sources, including blazars (both observed as targets

[13] https://heasarc.gsfc.nasa.gov/w3browse/all/milliquas.html

[14] https://heasarc.gsfc.nasa.gov/docs/software/lheasoft/

[15] https://heasarc.gsfc.nasa.gov/docs/heasarc/caldb/

of Swift observations and as serendipitous sources), other Swift targets, and a large number of serendipitous sources.

Some of the blazars observed by Swift are located in complex regions of the X-ray sky, where significant extended X-ray emission is present. These might be fields including bright clusters of galaxies or which suffer from residual contamination due to "bright Earth", that is, radiation reflected by the atmosphere when Swift points close to the Earth limb. Such fields can be very complex and certainly difficult to analyse in an automatic way or by inexperienced users. To remove this problem we applied a cleaning procedure that consisted of two checks:

1. **Background intensity consistent with expectations.** All fields where the measured background was found to be larger than 4σ compared to the average image background observed in all fields in the sample were flagged out.
2. **Number of detected point sources consistent with X-ray LogN-LogS.** To do that we built a 80x80 pixels sensitivity map based on local exposure, vignetting, and background. We then used this map and the LogN-LogS of Mateos et al. (2008) to calculate the expected number of cosmic extragalactic sources in the field. All X-ray images where the number of detected sources deviated more than 4σ from the expectations were flagged out.

This procedure lead to the identification of 353 observations ($\sim 3\%$ of the total) that suffer from significant background or apparent point-source excesses. All sources detected in these fields, including 74 blazars, have been removed from the final sample.

This process led to a "clean" sample including a total of 33,396 X-ray sources, with 8,896 detections of 2,308 distinct blazars comprising 770 FSRQs, 1,276 BL Lacs and 262 blazars of uncertain type.

Fig. 3 plots the observed count rate in the 0.3-10.0 keV band against exposure time of all the sources in the clean sample showing FSRQs in blue, BL Lacs in green and other targets and serendipitous sources in grey. The dotted horizontal line marks the count-rate limit above which pileup [16] becomes significant in sources observed in PC mode, causing significant flux underestimation and spectral distortion.

As can be seen from Fig. 3 most blazars are detected well above the minimum detectable count rate, and therefore with good statistics, as in most cases they were the target of the Swift observation. The red histogram overlaid on the plot represents the number of blazars included in each time bin. Three peaks at approximately 1, 2 and 4-5 ks are clearly visible, reflecting the Swift preferred exposure times for blazars.

The following scientific data products that match the operational definition of transparency given in Par. 1, are available.

1. A catalogue of XRT point sources called 1OUSXB, including the following
   - Count rates and X-ray fluxes in the 0.3-10.0 keV (full band), 0.3-1.0 keV (soft band), 1.0-2.0 keV (medium band), and the 2.0-10.0 keV (hard band).
   - Three sigma upper limits when a source is not detected in the soft, medium or hard energy band.
   - Three independent $\nu f(\nu)$ flux measurements, deabsorbed to correct for Galactic absorption and suitable for SED plotting, calculated at 0.5, 1.5 and 4.5 keV, from the count rates observed in the soft, medium and hard energy bands. These $\nu f(\nu)$ fluxes are available within the VOU-Blazars (Chang et al. 2019b) and the SSDC-SED[17] tools.
   - Power-law energy slope and one sigma statistical error, estimated from the hardness ratio, defined as (soft+medium band)/(hard band), only for sources detected with at least ≈ 50 net counts), and from a least-squares fit to the $\nu f(\nu)$ fluxes at 0.5, 1.5 and 4.5 keV.
   - A 3.0 keV $\nu f(\nu)$ flux point based on the count rate in the full band.
   - A $\nu f(\nu)$ flux at 1.0 keV, interpolated between the fluxes at 0.5 and 1.5 keV, suitable for light curve comparison with other X-ray satellites at the reference energy of 1.0 keV.
2. X-ray images in the full, soft, medium and hard energy bands. These images are provided in GIF format for easy inspection.
3. Co-added events files and associated-vignetting corrected exposure maps.
4. A ready-to-use Docker version of the *Swift-DeepSky* pipeline software, as well as the open source version.

The results and data products are available in a variety of ways: (i) as FITS and CSV formatted tables; (ii) as on-line interactive tables that, in addition to the parameters included in the FITS catalogue, give access to products such as images; (iii) as SED spectral data accessible via the VOU-SED and the SSDC SED tools, all of which are available from the http://openuniverse.asi.it portal, (iv) through a web query interface at vo.bsdc.icranet.org, and via Virtual Observatory services, (see http://openuniverse.asi.it/OUforBlazars for details). The table is also published through an IVOA cone search service (SCS[18]) and database graphical query interface provided by DaCHS (Demleitner et al. 2014) at http://vo.bsdc.icranet.org/ousxb/q/cone/form.

In addition, full radio to γ-ray SEDs for each blazar, including the data of the results presented here, can be generated from the Open Universe web portal at openuniverse.asi.it.

4.1. Blazars frequently monitored by Swift

A few bright and highly variable objects have been monitored by Swift-XRT, particularly during flares, with short observations performed on a daily basis. To avoid losing possible daily X-ray variability that was the objective of the frequent rate of observations for these sources we have run the *Swift-DeepSky* pipeline using a time interval of 1 day. The list of these intensely observed blazars and the total number of observations for each object is given in Table 1, where column 1 is the source name; column 2 is the number of XRT PC mode observations in one day with

[16] https://swift.gsfc.nasa.gov/analysis/xrt_swguide_v1_2.pdf

[17] https://tools.ssdc.asi.it/SED/

[18] http://www.ivoa.net/documents/latest/ConeSearch.html

exposure larger than 200 seconds; column 3 is the number of detections free of pileup; column 4 is the 0.3-10.0 keV median count rate; and column 5 is the 0.3-10.0 keV median absolute deviation about the median as a variability measure.

All the data products generated for the observations integrated over one week are also available for these shorter exposures.

Some well-known blazars such as MRK 421, MRK 501 and 3C 454.3 that have been monitored by Swift do not appear in table 1 since their X-ray fluxes are so high that the Swift-XRT observations were mostly made in WT mode; even when PC mode observations are available in the archive, these are very often subject to serious pileup. Detailed flux measurements, spectra and other high-transparency data products for these blazars will be published in a future paper presenting a systematic spectral analysis of WT and PC Swift XRT data of blazars (see Giommi 2015, for preliminary results) using the XSPEC package (Arnaud 1996).

5. Results: some examples

In this section we give some examples of the content of our catalogue and related data, and of how it can be used for multi-frequency, time variability, and multi-messenger analysis.

5.1. Sensitivity range

Fig. 4 plots the observed 0.3-10.0 keV energy flux vs exposure time, showing that the sensitivity of the Swift XRT data set considered ranges from $\sim 10^{-12}$ erg cm^{-2} s^{-1} for the very shortest ($\sim$ 200 seconds) exposures to $\sim 7 \times 10^{-15}$erg cm^{-2} s^{-1} for exposures as long as $\sim 10^5$ seconds. Sources detected with a 0.3-10.0 keV count rate larger than 0.6 cts/s are affected by pileup and are not plotted in this figure. For this reason the maximum flux in the sample of sources not flagged as affected by pileup is limited to $\sim 2-4 \times 10^{-11}$ erg cm^{-2} s^{-1}, depending on the spectral slope and the amount of absorption in the Galaxy (NH). This range of sensitivities is intermediate between that of the sources in the catalogue of D'Elia et al. (2013), who only considered single observation_IDs, and the lists of Evans et al. (2014); Puccetti et al. (2011), who instead stacked all the XRT data available.

5.2. Energy (SEDs) and time domain (light-curves) plots

Figure 5 shows the SED of BL Lacertae, the prototypical object of the blazar class. The grey points are non-simultaneous multi-frequency archival data showing the typical double-humped SED and large flux variations. The red points are 0.5, 1.5, 3.0 and 4.5 keV νf(ν) measurements from our catalogue. They show a hard spectrum and approximately a factor 10 intensity variability, the details of which are shown in Fig. 6 where the 0.3-10 keV X-ray flux (top panel) and the energy spectral slope (bottom panel), are plotted as a function of observation date.

Fig. 7 shows the SED of OJ 287, a blazar where the two SED components meet in the middle of the XRT energy band. The green points are spectral data obtained from the first XSPEC spectral analysis of all the XRT data in

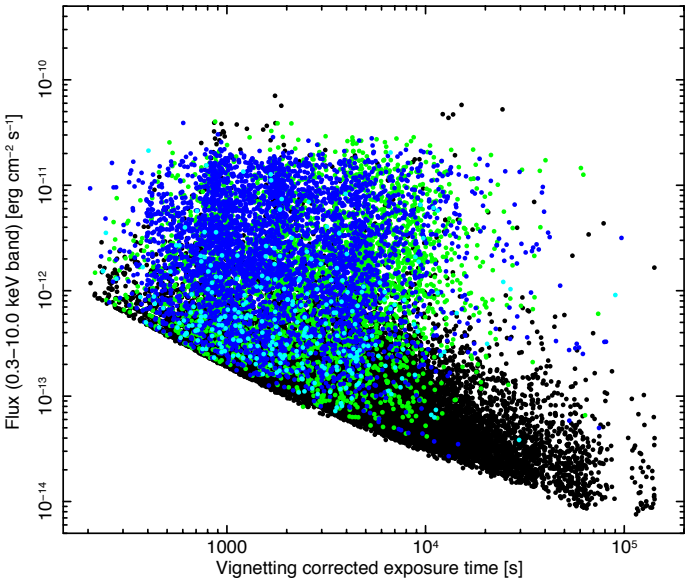


Fig. 4. 0.3-10.0 keV band flux versus vignetting-corrected exposure time for all detected sources free of pileup in PC mode (count rate< 0.6 cts/s). Colour coding as in Fig. 3.

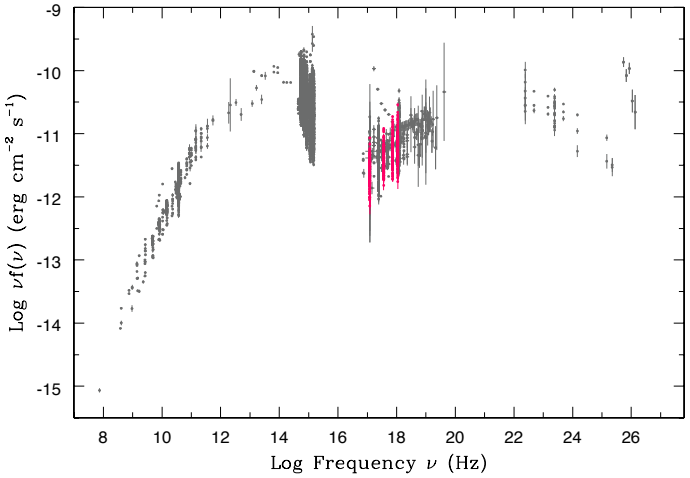


Fig. 5. Spectral Energy Distribution of BL Lacertae. Grey points are archival multi-frequency data. Red points are from this work.

PC and WT mode that was run on a sub-sample of bright blazars in 2015. The red points from this work do not reach the highest fluxes because of pileup problems above the count-rate of 0.6 ct/s. The top panel of figure 8 shows how the low energy flux (0.5 keV), at the end of the first SED component varies in a different way than the flux at 4.5 keV (middle panel), which belongs to the high energy SED component. The variation of the spectral slope is shown in the bottom panel.

5.3. The blazar TXS 0506+056: a likely source of IceCube neutrinos

One way to illustrate the reliability of our database is to compare our results to those published by independent authors on the same data set. We consider here the case of TXS 0506+056, the blazar that has been recently, and for the first time, associated to several IceCube neutrinos, and

Table 1. Blazars observed by Swift with short and frequent, mostly daily XRT exposures in PC mode.

Blazar name	no. of XRT observations[a]	no. of detections below pileup limit	⟨rate⟩[b] (cts s^{-1})	MAD[c] (%)
OJ 287	304	303	0.202	23.3
3C 279	282	261	0.355	17.5
PKS 1510-089	218	218	0.217	16.6
S5 0716+714	185	156	0.294	34.0
PG 1553+113	165	33	1.040	41.3
PKS 0235+164	158	155	0.048	40.5
PKS 0208-512	140	140	0.063	23.3
BZQJ 1635+3808	130	130	0.105	47.1
1ES 2344+514	126	64	0.599	26.7
PKS 0528+134	116	116	0.035	48.0
ON 231	113	112	0.057	25.8
CTA 102	110	89	0.322	50.9
1H 0323+342	108	88	0.426	23.7
MS 1207.9+3945	103	103	0.084	21.5
PKS 0921-213	94	94	0.216	19.9
NRAO 530	89	89	0.045	19.0
3C 66A	83	83	0.100	28.1
PKS 1222+216	73	73	0.111	22.2
TXS 0506+056[d]	49	49	0.053	23.5

[a] Integrated with one day time interval executed in PC mode with exposure time larger than 200 seconds
[b] Median count rate in the total $0.3-10$ keV band
[c] Median Absolute Deviation about the median count rate
[d] Blazar associated to the IceCube high-energy neutrino IC170922 and other IceCube neutrinos (Padovani et al. 2018).

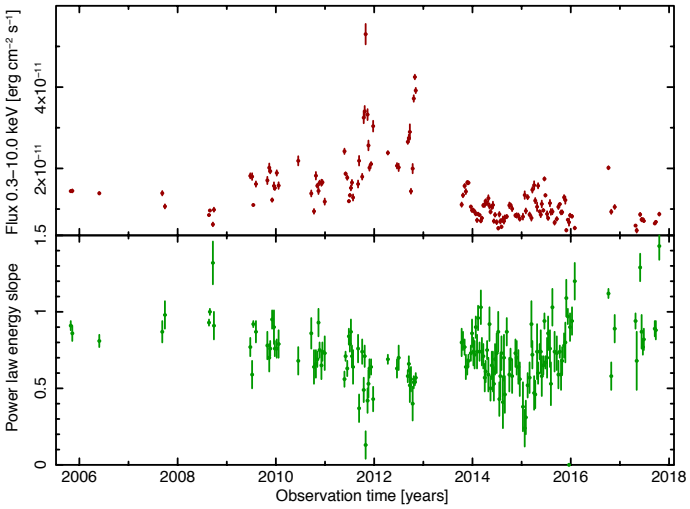


Fig. 6. History of the 0.3-10.0 keV band flux and estimated power-law energy spectral slope of BL Lacertae.

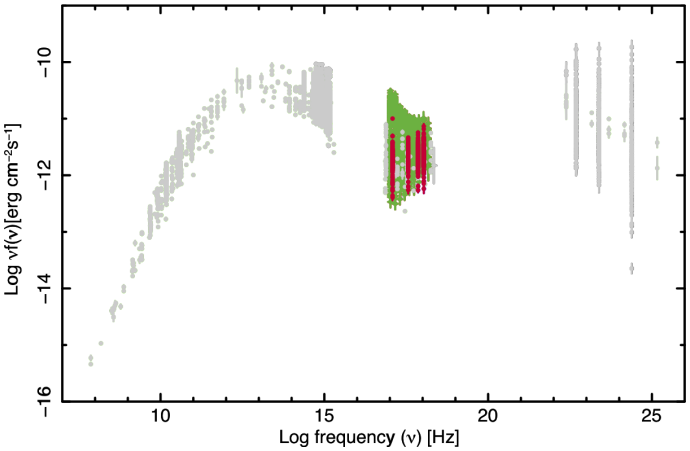


Fig. 7. Spectral Energy Distribution of the blazar OJ 287. Grey points are archival multi-frequency data. Red points are from this work (data in PC mode and count rate <0.6 cts/s). Green points are XSPEC spectra from the first analysis of all the XRT data in PC and WT mode run on a small sub-sample of blazars (Giommi 2015).

in particular to the high-energy neutrino IC170922. This source was observed by Swift a few hours after the neutrino arrival, and has been frequently monitored in the weeks after the IceCube event.

A complete analysis of the first two months of the Swift-XRT monitoring of TXS 0506+056 has been reported by Keivani et al. (2018). Fig. 9 plots the 0.3-10.0 keV and 2-10 keV bands, and the power-law photon index of this blazar as a function of time, based on the content of our database which, we recall, was built in a completely automated way and could have been produced by any user with the *Swift-DeepSky* Docker container. A detailed comparison of this figure with Fig. 2 and Table 1 of Keivani et al. (2018) clearly shows that our results are essentially identical to those of Keivani et al. (2018). Note that Fig. 9, in addition to the flux in the full band (red points in the upper panel) reported by Keivani et al. (2018), also plots as green points in the middle panel the flux in the hard 2-10 keV band. We have done this to show that the maximum source intensity in the two energy bands occurs at different times: immediately after the arrival of the neutrino in the hard band, when the spectrum was hardest, and at a later time in the full 0.3-10.0 keV band.

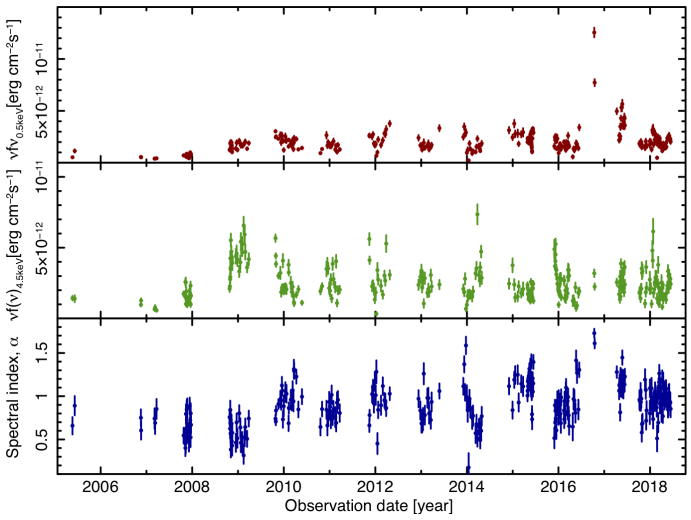


Fig. 8. The $\nu f(\nu)$ flux at 0.5, 4.5 keV and the power law energy spectral index of the blazar OJ 287 are plotted against observation date. Many differences in the top and middle panel are clearly visible. Note in particular that the X-ray flares occur in different periods in the soft (0.5 keV) and hard (4.5 keV) part of the X-ray spectrum.

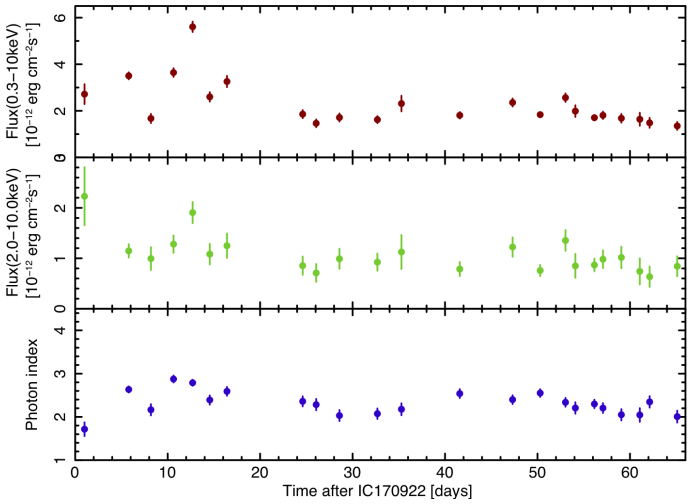


Fig. 9. The 0.3-10.0 keV and 2-10 keV band flux in units of 10^{-12}erg cm^{-2} s^{-1}(top and middle panel), and the power law photon index of TXS0506+056 (bottom panel) are plotted as a function of time. All uncertainties are one sigma.

5.4. Some population statistical properties

Fig. 10 shows the distributions of the power-law energy spectral indices in the sub-samples of FSRQs, BL Lacs and QSOs with no radio detection in the million quasar catalogue (MILLIQUAS Flesch 2015), that have been serendipitously detected in our X-ray images. The distributions are clearly distinct, reflecting the different ranges of synchrotron peak energies of the SED components in FSRQs and BL Lacs (see e.g. Giommi et al. 2012; Giommi et al. 2012) and the different X-ray emission process in radio-quiet QSOs that is due to accretion onto the super-massive black hole, rather than non-thermal emission from a relativistic jet. The spectral index distribution in sample of QSOs with no radio emission peaks at ∼0.8, as expected in this type of sources (e.g. Comastri et al. 1995).

Finally, Fig. 11 illustrates the difference between the redshift distributions of FSRQs with hard ($\alpha < 0.5$, solid red histogram) and with steeper ($\alpha > 0.5$, dotted black histogram) X-ray spectral slopes. A KS test gives a probability of $\sim 2. \times 10^{-7}$ that the two distributions come from the same parent population. The fact that the hard sources are statistically observed at higher redshifts could be due to different reasons, e.g.:

- a spectral hardening at energies above 10 keV that enters the XRT energy band (0.3-10.0 keV) only for high-redshift sources.
- a dependence of the X-ray spectral slope on luminosity, with the high-redshift and more powerful FSRQs showing the hardest spectra.
- the X-ray spectrum is the result of the superposition of two components, one that is relatively soft ($\alpha \sim 0.8$) due to accretion onto the super-massive black hole, and a second, much harder one that is due to the inverse-Compton emission from the jet. At relatively high energies (E $\gtrsim$ 10 keV) the hard component starts dominating the spectrum, which is red-shifted into the 0.3-10 keV XRT band for high redshift sources.

A detailed statistical study is needed to distinguish among the various possibilities.

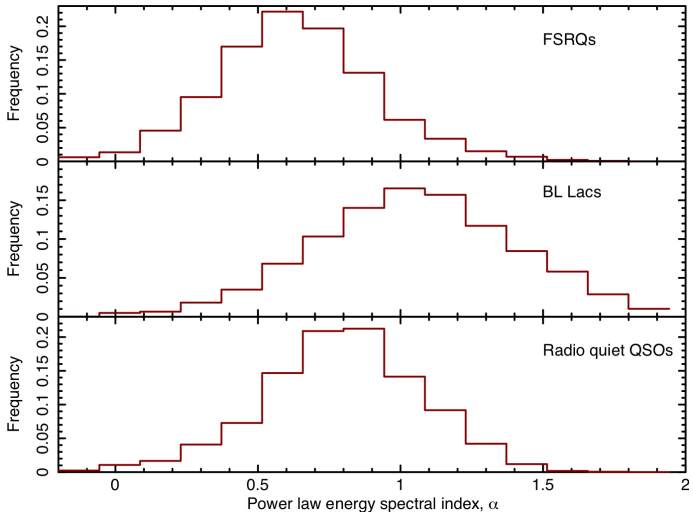


Fig. 10. The distribution of the power law energy spectral index in the sub-samples of FSRQs (top), BL Lacs (middle), and radio quiet QSOs (bottom).

5.5. Comparison with previous Swift-XRT catalogues

Other catalogues of point-like X-ray sources detected in Swift-XRT images have been published in the past, e.g. Puccetti et al. (2011); D'Elia et al. (2013); Evans et al. (2014). In addition to the coverage extension from 8 to 14 years of Swift observations, the approach followed in this paper is different in several ways:

- It has been designed to make all scientific products easily and readily accessible, in a number of ways (e.g. through VO access, the Open Universe portal, via SED tools, etc.).

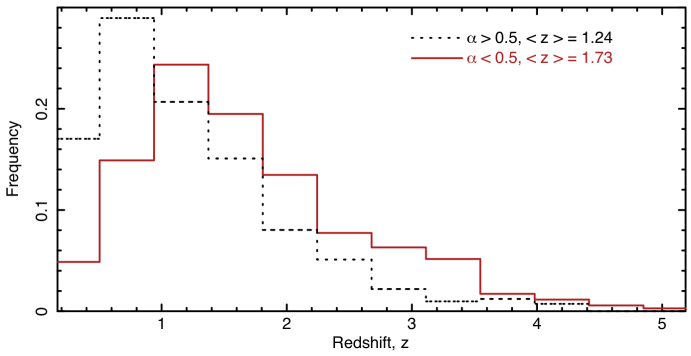


Fig. 11. The redshift distribution of FSRQs with different power law spectral indices (α). The black dotted histogram refers to objects with $\alpha > 0.5$ while the red solid histogram is for sources with $\alpha < 0.5$. FSRQs with flat spectral slopes tend to have larger redshifts.

– It demonstrates the possibility to extend the access to X-ray data analysis, and space science data in general, to non-experts, in principle to anyone interested in the field.
– It intends to support present and future gamma-ray surveys, in the context of the emerging field of multi-messenger astrophysics, by providing suitable blazar data from the most extensive X-ray mission of its kind. Scientific applications of this dataset could include: a) help in the identification of HE and VHE γ-ray sources, as well as high-energy neutrinos and possibly UHECRs astrophysical counterparts; b) support the selection of targets for VHE γ-ray observations; c) provide multi-temporal X-ray data suitable for the construction of time dependent SEDs to be compared to physical models, etc.

6. Open Universe for blazars: future developments

We intend to extend the work presented in this paper to other multi-frequency data on blazars. The following is a preliminary list of activities planned to be carried out in the coming months.

The Swift XRT data of blazars with more than 50 net counts in our database (about 1,000 objects), as well as all XRT data of bright blazars taken in both WT readout mode will be processed by means of an extended pipeline that takes into account and corrects for pileup problems, and generates X-ray spectra using the XSPEC package (Arnaud 1996). Early results from a test run of this processing, carried out on a small subset of very bright X-ray blazars, have been reported in Giommi (2015).

A similar procedure will be followed to analyse all public observations of blazars carried out with the hard X-ray observatory NuSTAR (Harrison et al. 2013).

Transparent-level results (νf(ν) spectra with 10 energy points) and high-level data products (pha spectra and response files) will also be made available in a number of ways including VOU-Blazars, the SSDC SED tool and other services available within the VO and the Open Universe portal.

As part of the Open Universe for blazars project, we are also producing, and will soon make available, Swift BAT spectra of the brightest X-ray blazars, and a set of adaptive-bin gamma-ray light-curves from Fermi-LAT data. These will be accessible, as with the other products, from the Open Universe portal, the VOU-Blazars and the SSDC SED tools, as well as via VO services. The temporal

Table 2. Details of the content of the 1OUSXB table in FITS format

Parameter	Description
Blazar name	Blazar name as it appears in Table 1 or in the 5BZCAT, 3LAC or 3HSP catalogue
Source name	catalogue source name formatted as 1OUSXBJhhmm.f+/-ddmm hhmm=hours, min of R.A., f=fraction of minutes ddmm=deg and min of Dec.
Other_name	alternative source name from literature when available
R.A.	Right Ascension in degrees (J2000.0)
Dec.	Declination in degrees (J2000.0)
MJD_Start	Modified Julian Day of observation start time
MJD_End	Modified Julian Day of observation end time
Exposure_time	Vignetting corrected exposure time[a]
Ctr_03_10	Count rate in the full (0.3-10.0 keV) band (cts s^{-1})
Ctr_03_10_error	1 sigma error on Ctr_03_10
Ctr_03_1	Count rate in the soft (0.3-1.0 keV) band (cts s^{-1})
Ctr_03_1_error	1 sigma error on Ctr_03_1
Ctr_03_1_UL	3 sigma upper limit[b] on Ctr_03_1
Ctr_1_2	Count rate in the medium (1.0-2.0) keV band (cts s
Ctr_1_2_error	1 sigma error on Ctr_1_2
Ctr_1_2_UL	3 sigma upper limit[b] on Ctr_1_2
Ctr_2_10	Count rate in the hard (2.0-10.0 keV) band (cts s^{-1})
Ctr_2_10_error	1 sigma error on Ctr_2_10
Ctr_2_10_UL	3 sigma upper limit[b] on Ctr_2_10
Flux_03_10	Observed energy flux in the full band (erg $cm^{-2}s^{-1}$)
Flux_03_10_error	1 sigma error on Flux_03_10
Flux_03_1	Observed energy flux in the soft band (erg $cm^{-2}s^{-1}$)
Flux_03_1_error	1 sigma error on Flux_03_1
Flux_03_1_UL	3 sigma upper limit[b] on Flux_03_1
Flux_1_2	Observed energy flux in the medium band (erg $cm^{-2}s^{-1}$)
Flux_1_2_error	1 sigma error on Flux_1_2
Flux_1_2_UL	3 sigma upper limit[b] on Flux_1_2
Flux_2_10	Observed energy flux in the hard band (erg $cm^{-2}s^{-1}$)
Flux_2_10_error	1 sigma error on Flux_2_10
Flux_2_10_UL	3 sigma upper limit[b] on Flux_2_10
Nufnu_3.0keV	absorption corrected[c] νf(ν) flux at 3.0 keV calculated from Ctr_03_10 (erg cm^{-2} s^{-1})
Nufnu_3.0keV_error	1 sigma error on Nufnu_3.0keV
Nufnu_0.5keV	absorption corrected[c] νf(ν) flux at 0.5 keV calculated from Ctr_03_1 (erg cm^{-2} s^{-1})
Nufnu_0.5keV_error	1 sigma error/3 sigma upper limit [d] on Nufnu_0.5keV
Nufnu_1.5keV	absorption corrected[c] νf(ν) flux at 1.5 keV calculated from Ctr_1_2 (erg cm^{-2} s^{-1})
Nufnu_1.5keV_error	1 sigma error/ 3 sigma upper limit [d] on Nufnu_1.5ke
Nufnu_4.5keV	absorption corrected[c] νf(ν) flux at 4.5 keV calculated from Ctr_2_10 (erg cm^{-2} s^{-1})
Nufnu_4.5keV_error	1 sigma error/ 3 sigma upper limit [d] on Nufnu_4.5ke
Nufnu_1.0keV	νf(ν) flux at 1.0 keV interpolated between Nufnu_0.5keV and Nufnu_1.5keV
Nufnu_1.0keV_error	1 sigma error on Nufnu_1.0keV
Spectral_slope	Power law energy spectral index
Spectral_slope_error	1 sigma error on Spectral_slope
Pileup flag	YES if Ctr_03_10 > 0.6 cts s^{-1}, NO otherwise

[a] Exposure time equivalent to that of an observation performed with the source exactly at the centre of the field of view.
[b] Upper limits are provided when no significant detection is achieved in the energy band considered.
[c] Galactic-absorption corrected flux in the observer frame.
[d] In case the source is not detected in this band, the Nufnu flux is set to 0 and the error is set equal to a three sigma upper limit

and spectral information will be combined to generate SED movies similar to the ones published in Padovani et al. (2018), and Giommi (2015), which are available on-line at https://www.youtube.com/embed/lFBciGIT0mE and http://youtu.be/nAZYcXcUGW8

6.1. An interactive database that is always up to date

One of the practical challenges in the provision of open data services in astronomy, especially when these involve operational satellites and aim at delivering high-level products in a timely manner, is to maintain the database up-to-date and conforming to the latest versions of the data analysis software and calibration files. Despite the practical difficulties involved in achieving this, such standards constitute an important step towards improving data transparency and in democratising the accessibility to the best quality scientific data available.

By taking advantage of new software technologies, it is possible today to minimise such shortcomings. In the current application of "Open Universe for Blazars" we have had recourse to the use of Linux containers based on Docker technology to test a new approach on data publication to enable users seamlessly to contribute to updating the public, worldwide available database of Swift observations. The effective goal is to have the table of Swift-DeepSky results always up-to-date with the latest observations taken by Swift. The container-based distributed analysis model means that the data processing and updating of the database will follow the actual user demand.

Such a service – *i.e.*, the software link between the pipeline and a central VO-enabled service equipped with an automated data publishing pipeline – is currently under internal commissioning. In the months to come such integration should become public, it will have no impact on the client side of *Swift-DeepSky*. The current automatic publication workflow under test will provide two versions of results table: the best-of-all sources (boa) table where each source appear only once – where the signal-to-noise ration *and* total exposure-time are maximum –, and the best-on-times sources (bot) table, where sources may appear more than once for different epochs.

7. Conclusion

We presented new sets of astronomical data products based on 14 years of Swift XRT observations of blazars. The associated results database includes flux measurements, spectral and timing information, as well as other high-level material that can be accessed through the Virtual Observatory, the Open Universe portal and in other ways. The pipeline software used to generate these data is also available in the form of an easy-to-use Docker container, which automatically downloads the low-level data and calibration necessary for the analysis, and can be run on all modern operating systems (Linux, Mac, Windows), thus removing platform dependencies and the need of any X-ray data analysis expertise.

Our approach significantly lowers technical barriers to X-ray data analysis, and introduces the possibility for anyone to reproduce the content of the database, extend it to other source types, or update it when new observations become available or when a new version of the software or calibration data are released. This is a major evolution compared to the traditional approach where astronomical catalogues are generated by teams of experts using complex hardware infrastructure and are issued at irregular time intervals, often separated by several years.

This paper advances, therefore, the first steps towards the implementation of a high-transparency, multi-frequency dynamic database service for the high-energy astrophysics community, which may become a particularly relevant resource in the emerging field of multi-messenger astronomy.

Following the principles of the Open Universe Initiative, this work is also meant to serve as a pathfinder to software solutions aiming to improve the usability of existing open space science data for a broader community of non-experts (scientists or otherwise) at a marginal cost. This is of particular importance in the context of the United Nations Sustainable Development Goals, as easy of access and transparency are key factors in the conversion of data into knowledge, and to achieve equal opportunities in the access of space science data and scientific information in general. Likewise, it is fully aligned with the mission of the United Nations Office for Outer Space Affairs (UNOOSA) in promoting international cooperation on the peaceful uses of outer space, and with the mandate of the Office following the UNISPACE conferences.

We encourage researchers, students, or anyone interested in X-ray astrophysics, to use this method and our software to build similar high-transparency scientific products for other types of astronomical sources.

Disclaimer. The views expressed herein are those of the authors and do not necessarily reflect the views of the United Nations.

Acknowledgements. **PG** acknowledges the support of the Technische Universität München - Institute for Advanced Studies, funded by the German Excellence Initiative (and the European Union Seventh Framework Programme under grant agreement no. 291763).

CHB acknowledges the support of ICRANet and the Brazilian government, funded by the CAPES Foundation, Ministry of Education of Brazil under the project BEX 15113-13-2.

UBdA acknowledges the support of a CNPq Productivity Reserach Grant no. 310827/2016-7 and the receipt of a FAPERJ Young Scientist Fellowship.

References

Ackermann, M., Ajello, M., Atwood, W. B., et al. 2015, ApJ, 810, 14
Arnaud, K. A. 1996, in Astronomical Society of the Pacific Conference Series, Vol. 101, Astronomical Data Analysis Software and Systems V, ed. G. H. Jacoby & J. Barnes, 17
Barthelmy, S. D., Barbier, L. M., Cummings, J. R., et al. 2005, Space Sci. Rev., 120, 143
Brandt, C. H., Giommi, P., Chang, Y. L., & et al. 2019, in preparation
Burrows, D. N., Hill, J. E., Nousek, J. A., et al. 2005, Space Sci. Rev., 120, 165
Chang, Y. L., Arsioli, B., Giommi, P., & Padovani P., Brandt, C. H. 2019a, A&A, submitted
Chang, Y. L., Brandt, C. H., & Giommi, P. 2019b, to be submitted
Comastri, A., Setti, G., Zamorani, G., & Hasinger, G. 1995, A&A, 296, 1
D'Elia, V., Perri, M., Puccetti, S., et al. 2013, A&A, 551, A142
Demleitner, M., M.C., N., Rothmaier, F., & Wambsganss, J. 2014, Astronomy and Computing
Evans, P. A., Osborne, J. P., Beardmore, A. P., et al. 2014, ApJS, 210, 8
Flesch, E. W. 2015, PASA, 32, e010
Gehrels, N., Chincarini, G., Giommi, P., et al. 2004, ApJ, 611, 1005
Giommi, P. 2015, Journal of High Energy Astrophysics, 7, 173

Giommi, P., Arrigo, G., Barres De Almeida, U., et al. 2018, arXiv e-prints
Giommi, P., Padovani, P., Polenta, G., et al. 2012, MNRAS, 420, 2899
Giommi, P., Polenta, G., Lähteenmäki, A., et al. 2012, A&A, 541, A160
Harrison, F. A., Craig, W. W., Christensen, F. E., et al. 2013, ApJ, 770, 103
IceCube Collaboration, Aartsen, M. G., Ackermann, M., et al. 2018, Science, 361, 147
Keivani, A., Murase, K., Petropoulou, M., et al. 2018, ApJ, 864, 84
Mannheim, K. 1995, Astroparticle Physics, 3, 295
Massaro, E., Maselli, A., Leto, C., et al. 2015, Ap&SS, 357, 75
Mateos, S., Warwick, R. S., Carrera, F. J., et al. 2008, A&A, 492, 51
Padovani, P., Alexander, D. M., Assef, R. J., et al. 2017, A&A Rev., 25, 2
Padovani, P., Giommi, P., Resconi, E., et al. 2018, MNRAS, 480, 192
Pollock, A. M. T. 2018, Space Research Today, 201, 15
Puccetti, S., Capalbi, M., Giommi, P., et al. 2011, A&A, 528, A122
Resconi, E., Coenders, S., Padovani, P., Giommi, P., & Caccianiga, L. 2017, MNRAS, 468, 597
Roming, P. W. A., Kennedy, T. E., Mason, K. O., et al. 2005, Space Sci. Rev., 120, 95
Urry, C. M. & Padovani, P. 1995, PASP, 107, 803
Wilkinson, M. D., Dumontier, M., Aalbersberg, I. J., et al. 2016, Scientific data, 3

Appendix A: The Swift-DeepSky pipeline

Swift-DeepSky is a software pipeline built on top of the Swift X-Ray Telescope Data Analysis Software (XRTDAS), designed and developed under the responsibility of the Space Science Data Center (SSDC) of the Italian Space Agency (ASI) and distributed within the NASA HEASoft[19] data reduction package and related Swift-XRT calibration files (CALDB)[20], that performs a complete X-ray image analysis of Swift XRT data. A detailed description of the pipeline is given in Brandt et al. 2019 (in preparation); in this appendix we outline the main features.

Swift-DeepSky executes in sequence the following main tasks

1. Retrieve the list of all observation_ID performed by Swift in the chosen period and select those executed in PC mode with exposure time larger than 200 seconds;
2. Download the data and calibration files that are necessary for the analysis from one of the Swift official archives;
3. Build exposure maps for every observation_ID;
4. Add exposure maps and event files if more than a single observation_ID has been performed in the chosen period (one week in this paper);
5. The XIMAGE tool reads the event list and exposure map, builds X-ray images in the full 0.3-10.0 keV band;
6. The XIMAGE/DETECT command searches the X-ray image for pointlike sources;
7. XIMAGE estimates the background in four energy intervals: the full band (0.3-10.0 keV), the soft (0.3-1.0 keV), medium (1.0-2.0 keV) and hard band (2.0-10.0 keV);
8. For every detected source in the full band, the XIMAGE/SOSTA tool estimates count-rates in all bands for all sources found by DETECT, and calculates three sigma upper limits in case a source is below the detection threshold;
9. NH command is run to estimate the amount of Galactic Hydrogen column in the direction of the source;
10. An estimate of a power law spectral slope is obtained by inverting count-rate ratio in the soft+medium and in the hard band;
11. Fluxes in all energy bands are calculated on the basis of count rates and NH assuming a power law spectrum with slope estimated from the hardness ratio or assuming an energy index of 0.8 for sources with less than ∼50 net counts;
12. Galactic absorption corrected $\nu f(\nu)$ fluxes, suitable for SED plotting are calculated from the counts estimated in the soft, medium and hard band, and from the full band;
13. A second value of the power law spectral slope is estimated by means of a linear least square fit to the 0.5, 1.5 and 4.5 keV $\nu f(\nu)$ fluxes;
14. If requested all the products are uploaded to a central database and made publicly available.

The *Swift-DeepSky* is open source, available at

– https://github.com/chbrandt/swift_deepsky.

The software is available encapsulated in a Docker container that can be run on MacOS, Linux and Windows10 operating systems, to improve and simplify usability.

The typical input to the pipeline is a position in the sky, right ascension and declination (in degrees), or the name of the object of interest (which will be resolved in real-time through Simbad[21]. E.g.,

```
# swift_deepsky --ra 317.58788 --dec -86.2894
```

, and also very useful is the filtering for observations within a time window:

```
# swift_deepsky --object 3c279 \
                --start 01/06/2018 \
                --end 31/12/2018
```

The default search radius the pipeline considers is 12 *arcmin*, approximately Swift's field-of-view; this value can be changed.

If the period of interest is not specified, all the exposures taken by Swift ever since its lifetime on the specified area of sky will be co-added.

To download the *Swift-DeepSky* Docker container the reader can follow the link "Open Software" from the Open Universe portal (openuniverse.asi.it) on the grey toolbar at the top of the web page and then on "OU-Swift_deepsky", or directly from:

– https://hub.docker.com/r/chbrandt/swift_deepsky

where full details on how to run it can be found.

The Docker version of the *Swift-DeepSky* pipeline can be considered a "high-transparency" X-ray data analysis software tool because a) it can be downloaded and installed in a few clicks, b) it removes platform dependencies and the need to download the data and calibration files from the archive, and c) it lowers the barrier to X-ray data analysis enabling users, with or without experience in Swift-XRT data analysis, to run data reduction software that generates reliable science-ready standard data products usable by everyone.

[19] https://heasarc.gsfc.nasa.gov/docs/software/lheasoft/
[20] https://heasarc.gsfc.nasa.gov/docs/heasarc/caldb/
[21] http://simbad.u-strasbg.fr/simbad/sim-fid